

OPEN MODELS CAN SILENTLY UNDERMINE PRIVACY: CONTEXT INFERENCE ATTACKS WITHOUT JAILBREAKS

000
001
002
003
004
005 **Anonymous authors**
006 Paper under double-blind review
007
008
009
010
011
012
013
014
015
016
017
018
019
020
021
022
023
024
025
026
027
028
029
030
031
032
033
034
035
036
037
038
039
040
041
042
043
044
045
046
047
048
049
050
051
052
053
054
055
056
057
058
059
060
061
062
063
064
065
066
067
068
069
070
071
072
073
074
075
076
077
078
079
080
081
082
083
084
085
086
087
088
089
090
091
092
093
094
095
096
097
098
099
100
101
102
103
104
105
106
107
108
109
110
111
112
113
114
115
116
117
118
119
120
121
122
123
124
125
126
127
128
129
130
131
132
133
134
135
136
137
138
139
140
141
142
143
144
145
146
147
148
149
150
151
152
153
154
155
156
157
158
159
160
161
162
163
164
165
166
167
168
169
170
171
172
173
174
175
176
177
178
179
180
181
182
183
184
185
186
187
188
189
190
191
192
193
194
195
196
197
198
199
200
201
202
203
204
205
206
207
208
209
210
211
212
213
214
215
216
217
218
219
220
221
222
223
224
225
226
227
228
229
230
231
232
233
234
235
236
237
238
239
240
241
242
243
244
245
246
247
248
249
250
251
252
253
254
255
256
257
258
259
260
261
262
263
264
265
266
267
268
269
270
271
272
273
274
275
276
277
278
279
280
281
282
283
284
285
286
287
288
289
290
291
292
293
294
295
296
297
298
299
300
301
302
303
304
305
306
307
308
309
310
311
312
313
314
315
316
317
318
319
320
321
322
323
324
325
326
327
328
329
330
331
332
333
334
335
336
337
338
339
340
341
342
343
344
345
346
347
348
349
350
351
352
353
354
355
356
357
358
359
360
361
362
363
364
365
366
367
368
369
370
371
372
373
374
375
376
377
378
379
380
381
382
383
384
385
386
387
388
389
390
391
392
393
394
395
396
397
398
399
400
401
402
403
404
405
406
407
408
409
410
411
412
413
414
415
416
417
418
419
420
421
422
423
424
425
426
427
428
429
430
431
432
433
434
435
436
437
438
439
440
441
442
443
444
445
446
447
448
449
450
451
452
453
454
455
456
457
458
459
460
461
462
463
464
465
466
467
468
469
470
471
472
473
474
475
476
477
478
479
480
481
482
483
484
485
486
487
488
489
490
491
492
493
494
495
496
497
498
499
500
501
502
503
504
505
506
507
508
509
510
511
512
513
514
515
516
517
518
519
520
521
522
523
524
525
526
527
528
529
530
531
532
533
534
535
536
537
538
539
540
541
542
543
544
545
546
547
548
549
550
551
552
553
554
555
556
557
558
559
559
560
561
562
563
564
565
566
567
568
569
569
570
571
572
573
574
575
576
577
578
579
579
580
581
582
583
584
585
586
587
588
589
589
590
591
592
593
594
595
596
597
598
599
599
600
601
602
603
604
605
606
607
608
609
609
610
611
612
613
614
615
616
617
618
619
619
620
621
622
623
624
625
626
627
628
629
629
630
631
632
633
634
635
636
637
638
639
639
640
641
642
643
644
645
646
647
648
649
649
650
651
652
653
654
655
656
657
658
659
659
660
661
662
663
664
665
666
667
668
669
669
670
671
672
673
674
675
676
677
678
679
679
680
681
682
683
684
685
686
687
688
689
689
690
691
692
693
694
695
696
697
698
699
699
700
701
702
703
704
705
706
707
708
709
709
710
711
712
713
714
715
716
717
718
719
719
720
721
722
723
724
725
726
727
728
729
729
730
731
732
733
734
735
736
737
738
739
739
740
741
742
743
744
745
746
747
748
749
749
750
751
752
753
754
755
756
757
758
759
759
760
761
762
763
764
765
766
767
768
769
769
770
771
772
773
774
775
776
777
778
779
779
780
781
782
783
784
785
786
787
788
789
789
790
791
792
793
794
795
796
797
798
799
799
800
801
802
803
804
805
806
807
808
809
809
810
811
812
813
814
815
816
817
818
819
819
820
821
822
823
824
825
826
827
828
829
829
830
831
832
833
834
835
836
837
838
839
839
840
841
842
843
844
845
846
847
848
849
849
850
851
852
853
854
855
856
857
858
859
859
860
861
862
863
864
865
866
867
868
869
869
870
871
872
873
874
875
876
877
878
879
879
880
881
882
883
884
885
886
887
888
889
889
890
891
892
893
894
895
896
897
898
899
900
901
902
903
904
905
906
907
908
909
909
910
911
912
913
914
915
916
917
918
919
919
920
921
922
923
924
925
926
927
928
929
929
930
931
932
933
934
935
936
937
938
939
939
940
941
942
943
944
945
946
947
948
949
949
950
951
952
953
954
955
956
957
958
959
959
960
961
962
963
964
965
966
967
968
969
969
970
971
972
973
974
975
976
977
978
979
979
980
981
982
983
984
985
986
987
988
989
989
990
991
992
993
994
995
996
997
998
999
1000
1001
1002
1003
1004
1005
1006
1007
1008
1009
1009
1010
1011
1012
1013
1014
1015
1016
1017
1018
1019
1019
1020
1021
1022
1023
1024
1025
1026
1027
1028
1029
1029
1030
1031
1032
1033
1034
1035
1036
1037
1038
1039
1040
1041
1042
1043
1044
1045
1046
1047
1048
1049
1050
1051
1052
1053
1054
1055
1056
1057
1058
1059
1059
1060
1061
1062
1063
1064
1065
1066
1067
1068
1069
1069
1070
1071
1072
1073
1074
1075
1076
1077
1078
1079
1079
1080
1081
1082
1083
1084
1085
1086
1087
1088
1089
1089
1090
1091
1092
1093
1094
1095
1096
1097
1098
1099
1099
1100
1101
1102
1103
1104
1105
1106
1107
1108
1109
1109
1110
1111
1112
1113
1114
1115
1116
1117
1118
1119
1119
1120
1121
1122
1123
1124
1125
1126
1127
1128
1129
1129
1130
1131
1132
1133
1134
1135
1136
1137
1138
1139
1139
1140
1141
1142
1143
1144
1145
1146
1147
1148
1149
1149
1150
1151
1152
1153
1154
1155
1156
1157
1158
1159
1159
1160
1161
1162
1163
1164
1165
1166
1167
1168
1169
1169
1170
1171
1172
1173
1174
1175
1176
1177
1178
1179
1179
1180
1181
1182
1183
1184
1185
1186
1187
1188
1189
1189
1190
1191
1192
1193
1194
1195
1196
1197
1198
1199
1199
1200
1201
1202
1203
1204
1205
1206
1207
1208
1209
1209
1210
1211
1212
1213
1214
1215
1216
1217
1218
1219
1219
1220
1221
1222
1223
1224
1225
1226
1227
1228
1229
1229
1230
1231
1232
1233
1234
1235
1236
1237
1238
1239
1239
1240
1241
1242
1243
1244
1245
1246
1247
1248
1249
1249
1250
1251
1252
1253
1254
1255
1256
1257
1258
1259
1259
1260
1261
1262
1263
1264
1265
1266
1267
1268
1269
1269
1270
1271
1272
1273
1274
1275
1276
1277
1278
1279
1279
1280
1281
1282
1283
1284
1285
1286
1287
1288
1289
1289
1290
1291
1292
1293
1294
1295
1296
1297
1298
1299
1299
1300
1301
1302
1303
1304
1305
1306
1307
1308
1309
1309
1310
1311
1312
1313
1314
1315
1316
1317
1318
1319
1319
1320
1321
1322
1323
1324
1325
1326
1327
1328
1329
1329
1330
1331
1332
1333
1334
1335
1336
1337
1338
1339
1339
1340
1341
1342
1343
1344
1345
1346
1347
1348
1349
1349
1350
1351
1352
1353
1354
1355
1356
1357
1358
1359
1359
1360
1361
1362
1363
1364
1365
1366
1367
1368
1369
1369
1370
1371
1372
1373
1374
1375
1376
1377
1378
1379
1379
1380
1381
1382
1383
1384
1385
1386
1387
1388
1389
1389
1390
1391
1392
1393
1394
1395
1396
1397
1398
1399
1399
1400
1401
1402
1403
1404
1405
1406
1407
1408
1409
1409
1410
1411
1412
1413
1414
1415
1416
1417
1418
1419
1419
1420
1421
1422
1423
1424
1425
1426
1427
1428
1429
1429
1430
1431
1432
1433
1434
1435
1436
1437
1438
1439
1439
1440
1441
1442
1443
1444
1445
1446
1447
1448
1449
1449
1450
1451
1452
1453
1454
1455
1456
1457
1458
1459
1459
1460
1461
1462
1463
1464
1465
1466
1467
1468
1469
1469
1470
1471
1472
1473
1474
1475
1476
1477
1478
1479
1479
1480
1481
1482
1483
1484
1485
1486
1487
1488
1489
1489
1490
1491
1492
1493
1494
1495
1496
1497
1498
1499
1499
1500
1501
1502
1503
1504
1505
1506
1507
1508
1509
1509
1510
1511
1512
1513
1514
1515
1516
1517
1518
1519
1519
1520
1521
1522
1523
1524
1525
1526
1527
1528
1529
1529
1530
1531
1532
1533
1534
1535
1536
1537
1538
1539
1539
1540
1541
1542
1543
1544
1545
1546
1547
1548
1549
1549
1550
1551
1552
1553
1554
1555
1556
1557
1558
1559
1559
1560
1561
1562
1563
1564
1565
1566
1567
1568
1569
1569
1570
1571
1572
1573
1574
1575
1576
1577
1578
1579
1579
1580
1581
1582
1583
1584
1585
1586
1587
1588
1589
1589
1590
1591
1592
1593
1594
1595
1596
1597
1598
1599
1599
1600
1601
1602
1603
1604
1605
1606
1607
1608
1609
1609
1610
1611
1612
1613
1614
1615
1616
1617
1618
1619
1619
1620
1621
1622
1623
1624
1625
1626
1627
1628
1629
1629
1630
1631
1632
1633
1634
1635
1636
1637
1638
1639
1639
1640
1641
1642
1643
1644
1645
1646
1647
1648
1649
1649
1650
1651
1652
1653
1654
1655
1656
1657
1658
1659
1659
1660
1661
1662
1663
1664
1665
1666
1667
1668
1669
1669
1670
1671
1672
1673
1674
1675
1676
1677
1678
1679
1679
1680
1681
1682
1683
1684
1685
1686
1687
1688
1689
1689
1690
1691
1692
1693
1694
1695
1696
1697
1698
1699
1699
1700
1701
1702
1703
1704
1705
1706
1707
1708
1709
1709
1710
1711
1712
1713
1714
1715
1716
1717
1718
1719
1719
1720
1721
1722
1723
1724
1725
1726
1727
1728
1729
1729
1730
1731
1732
1733
1734
1735
1736
1737
1738
1739
1739
1740
1741
1742
1743
1744
1745
1746
1747
1748
1749
1749
1750
1751
1752
1753
1754
1755
1756
1757
1758
1759
1759
1760
1761
1762
1763
1764
1765
1766
1767
1768
1769
1769
1770
1771
1772
1773
1774
1775
1776
1777
1778
1779
1779
1780
1781
1782
1783
1784
1785
1786
1787
1788
1789
1789
1790
1791
1792
1793
1794
1795
1796
1797
1798
1799
1799
1800
1801
1802
1803
1804
1805
1806
1807
1808
1809
1809
1810
1811
1812
1813
1814
1815
1816
1817
1818
1819
1819
1820
1821
1822
1823
1824
1825
1826
1827
1828
1829
1829
1830
1831
1832
1833
1834
1835
1836
1837
1838
1839
1839
1840
1841
1842
1843
1844
1845
1846
1847
1848
1849
1849
1850
1851
1852
1853
1854
1855
1856
1857
1858
1859
1859
1860
1861
1862
1863
1864
1865
1866
1867
1868
1869
1869
1870
1871
1872
1873
1874
1875
1876
1877
1878
1879
1879
1880
1881
1882
1883
1884
1885
1886
1887
1888
1889
1889
1890
1891
1892
1893
1894
1895
1896
1897
1898
1899
1899
1900
1901
1902
1903
1904
1905
1906
1907
1908
1909
1909
1910
1911
1912
1913
1914
1915<br

054 Defenses against inference-time context leakage are still limited and fragmented. Broadly, they can be
 055 divided into two categories. Instruction-based defenses (Zhou et al., 2022) aim to prevent disclosure
 056 by refusing to answer certain queries or excluding sensitive spans from the output. Filtering-based
 057 defenses (Zhang & Ippolito, 2023) rely on an auxiliary model to scan and block outputs mentioning
 058 PII. Both approaches depend on the sensitive content being explicitly present in the output (verbatim
 059 or encoded, e.g. Base64). They do not address cases where information is only revealed indirectly
 060 through distributional shifts in the model’s responses.

061 In this paper, we demonstrate a new vulnerability: a *context inference attack* that infers secrets
 062 embedded in system prompts without relying on direct jailbreaking techniques. We frame this
 063 as a membership inference problem: given a candidate set of secrets, an adversary issues queries
 064 to the target model, observes its responses, and uses a surrogate model to evaluate which secret
 065 best explains the observed behavior. The key insight is that even benign queries elicit response
 066 patterns subtly shaped by the hidden secret. By aggregating evidence across multiple queries, the
 067 adversary can reliably identify the true secret. Unlike adversarial prompts, our queries are random
 068 and non-malicious, making them difficult to block via input filtering.

069 We further study how to select effective probing queries. We propose an online DPO (Rafailov et al.,
 070 2023)-based generator that optimizes queries for maximum inference accuracy, and we compare it
 071 with prompt-tuning (Lester et al., 2021) approaches that generate more adversarial queries but are
 072 easier to detect. Our attack applies broadly to both LLMs and VLMs. We evaluate on three Qwen2.5-
 073 Instruct LLMs (Yang et al., 2024), two LLaVA VLMs (Liu et al., 2023), and two Qwen2.5VL
 074 VLMs (Bai et al., 2025). In experiments, optimized queries achieve attack success rates of up to 100%
 075 across models and remain effective under instruction-based defenses. Moreover, queries optimized
 076 on smaller surrogates transfer successfully to larger related models, confirming the practicality of our
 077 approach.

078 Finally, we summarize our contributions as follows:

- 079 • We identify and formalize **context inference attacks**, showing how sensitive information
 080 embedded in system prompts can be inferred without explicit leakage.
- 081 • We develop a **likelihood-based inference method** that leverages surrogate models and
 082 benign queries to recover secrets from contextual prompts.
- 083 • We introduce **query optimization strategies** based on online DPO and prompt tuning, and
 084 analyze their effectiveness under instruction-based defenses.
- 085 • We provide an extensive **empirical evaluation** on both LLMs and VLMs, demonstrating
 086 high success rates and strong transferability across model families and sizes.

089 2 BACKGROUND

091 **Generative Models and Sampling.** A Large Generative Model (LGM) θ defines a probability
 092 distribution over a vocabulary \mathcal{V} . Given a context prefix p , the model outputs logits $\text{Logits}(p) \in \mathbb{R}^{|\mathcal{V}|}$.
 093 These are converted into the next-token probability distribution $\mathbb{P}(\cdot|p; \mathcal{T})$ using temperature scaling
 094 ($\mathcal{T} > 0$) and the softmax function:

$$095 \quad \mathbb{P}(v|p; \mathcal{T}) = \frac{\exp(\text{Logits}(p, v)/\mathcal{T})}{\sum_{v' \in \mathcal{V}} \exp(\text{Logits}(p, v')/\mathcal{T})} \quad \forall v \in \mathcal{V} \quad (1)$$

098 Temperature controls the distribution’s sharpness and text generation $\text{Generate}(p; \theta, \mathcal{T})$ proceeds
 099 autoregressively by sampling a token v_t from $\mathbb{P}(\cdot|p \cdot v_{1:t-1}; \mathcal{T})$ at each step t until an end-of-sentence
 100 (EoS) token is sampled. Common sampling strategies include top-k sampling, which selects the top-k
 101 most likely next tokens.

102 **Negative Log Likelihood.** Negative Log Likelihood (NLL) measures how well the model’s pre-
 103 dicted probability distribution matches the target data. If a model θ predicts the sequence $Y = y_{1:T}$
 104 given input X , then the Negative Log-Likelihood (NLL) is:

$$106 \quad \text{NLL}(Y|X; \theta) = -\log P_\theta(Y|X) = -\sum_{t=1}^T \log P_\theta(y_t|y_{<t}, X).$$

108 Lower NLL indicates the model assigns higher probability to the observed sequence, suggesting a
 109 better fit.
 110

111
 112 **System Prompts.** Beyond the immediate user input (user prompts), Large Language Models
 113 (LLMs) can be guided by *system prompts*. These are persistent instructions, often hidden from the
 114 end-user, that define the model’s persona, enforce safety guidelines, or provide context relevant across
 115 an entire interaction session. In our work, distinct system prompts represent the different underlying
 116 conditions (*e.g.*, containing secret A or secret B) whose effects on the model’s output distributions
 117 we aim to distinguish.
 118

119 **Teacher Forcing.** Standard text generation involves *autoregressive sampling*, where the model’s
 120 prediction at step t is conditioned on its own sampled outputs from steps 1 to $t - 1$. In contrast,
 121 *teacher forcing* is a technique primarily used during training or analysis. When evaluating a sequence
 122 $v_{1:T}$, teacher forcing provides the ground-truth token v_{t-1} as input to predict the distribution for
 123 token v_t , regardless of what the model might have predicted at step $t - 1$. This allows for a controlled
 124 analysis of the model’s next-token predictions $P_\theta(\cdot | p \cdot v_{1:t-1})$ conditioned on a specific, fixed prefix
 125 $p \cdot v_{1:t-1}$. We utilize teacher forcing to obtain comparable output probability distributions from
 126 models operating under different system prompts (A vs. B) for the exact same reference sequence.
 127

128 3 THREAT MODEL AND SECURITY GAMES DEFINITION

129 3.1 THREAT MODEL

130 We consider scenarios where a language model provider operates an LGM with parameters θ , that
 131 processes hidden contextual information potentially containing sensitive secrets s^* . This hidden
 132 context could be part of a system prompt containing proprietary instructions or API keys, or data
 133 retrieved via methods like Retrieval-Augmented Generation (RAG) containing Personally Identifiable
 134 Information (PII) or other private details. The provider aims to leverage this context for utility while
 135 preventing its leakage to potentially adversarial users. We formalize the interaction and capabilities
 136 below.
 137

138 **Provider (Defender).** The provider operates the target LGM θ with white-box access, enabling
 139 fine-tuning or instruction-tuning (*model control*). To prevent leakage, the provider can hide the
 140 context $C(s^*)$ during generation so that the secret s^* is never exposed to the user (*context hiding*).
 141 Furthermore, generated responses \mathcal{R}_i can be monitored and filtered to scrub sensitive information
 142 before being returned (*output filtering*). The provider also manages users through mechanisms such
 143 as rate limiting, authentication, and banning suspected attackers, with each user limited to at most
 144 K queries (*user management*). Finally, the provider retains control over the randomness in text
 145 generation, such as the sampling process, keeping it secret to increase robustness against attacks
 146 (*randomization*).
 147

148 **Attacker (Adversary) \mathcal{A} .** The primary *goal* of the adversary is to infer the hidden secret s^* . We
 149 formalize this as the Secret Inference (SI) setting (Definition 1), where the attacker is given a known
 150 finite set of possible secrets $\mathcal{S} = \{s_1, s_2, \dots, s_n\}$ and aims to identify which specific $s^* \in \mathcal{S}$ is used
 151 by the provider. Knowing \mathcal{S} means that the attacker is aware of the complete candidate set from
 152 which the secret is drawn, but does not know which secret is actually selected.
 153

154 The adversary interacts with the provider’s LGM via black-box API queries (*interaction*), sending
 155 up to K queries $\mathcal{Q}^K = \{Q_i\}_{i=1}^K$ and receiving the corresponding responses $\mathcal{R}^K = \{R_i\}_{i=1}^K$, where
 156 $\mathcal{R}_i \leftarrow \text{Generate}(C(s^*) || Q_i; \theta)$. Regarding *model access*, the attacker may operate in a white-box
 157 setting, where θ is fully known but cannot be modified (*e.g.*, an open-source model), or in a black-box
 158 setting, where the attacker uses a surrogate model $\hat{\theta}$ that approximates θ (we later quantify this
 159 approximation in Assumption 1.). Finally, the attacker is assumed to know the context hiding function
 160 $C(\cdot)$ (*knowledge of context template*), *i.e.*, the template or structure used to incorporate the secret into
 161 the input, while the actual secret s^* remains unknown.

162 3.2 SECURITY GAMES FOR CONTEXT INFERENCE
163

164 To formally analyze the security of language models against context inference, we define a security
165 game capturing the goal of the adversary. In this game, an adversary \mathcal{A} interacts with a challenger
166 \mathcal{O} who has access to the target model θ and a secret context s^* . The adversary has a budget of K
167 queries.

168 **Definition 1** (Secret Inference Game). *Let θ be the target LGM and $C(\cdot)$ the context formatting
169 function, and let \mathcal{S} be a finite set of possible secrets known to the adversary. In the Secret Inference
170 game $\mathbf{Game}_{\mathcal{A}}(\mathcal{S}, \theta)$, the challenger \mathcal{O} first samples a secret $s^* \leftarrow \mathcal{S}$ uniformly at random (setup).
171 During the query phase, the adversary \mathcal{A} , given \mathcal{S} , adaptively issues up to K queries \mathcal{Q}^K to the
172 challenger, who responds with $R_i \leftarrow \text{Generate}(C(s^*) \parallel Q_i; \theta)$ for each query. Finally, the adversary
173 outputs a guess $\hat{s} \in \mathcal{S}$ and is considered to win the game if $\hat{s} = s^*$ (winning condition).*

174 The advantage of an adversary \mathcal{A} in this game is defined as:
175

$$176 \mathbf{Adv}_{\mathcal{A}}(\mathcal{S}, \theta) = \Pr[\hat{s} = s^*] - \frac{1}{|\mathcal{S}|}.$$

177 A model θ is considered (t, K, ϵ) -secure against secret inference for the set \mathcal{S} if no adversary \mathcal{A}
178 running in time at most t and query budget K can achieve $\mathbf{Adv}_{\mathcal{A}}(\mathcal{S}, \theta) > \epsilon$.

179 Definition 1 captures the scenario where the attacker knows the possible secrets and aims to identify
180 the specific one used by the provider. The advantage measures how much better the adversary
181 performs than random guessing.

182 4 CONCEPTUAL APPROACH
183

184 We now describe a context inference attack that consists of sending K benign queries \mathcal{Q}^K to the
185 provider’s LGM, which returns K responses \mathcal{R}^K . Given these responses, our goal is to find an attack
186 method $\mathcal{A}(\mathcal{Q}^K, \mathcal{R}^K, \theta)$ that optimizes $\Pr[s^* = \mathcal{A}(\mathcal{Q}^K, \mathcal{R}^K, \theta)]$. We use a Maximum Likelihood
187 Estimation method for our attack to infer the *true* secret $s^* \in \mathcal{S}$. Additionally, our attack is also
188 dependent on the choice of query and therefore we provide a query optimization algorithm to find K
189 queries \mathcal{Q} that maximize our attack’s success rate at inferring the correct secret.

190 4.1 MAXIMUM LIKELIHOOD ESTIMATION ATTACK
191

192 We consider an attacker aiming to infer a hidden secret $s^* \in \mathcal{S}$ used by a provider’s model θ . The
193 attacker possesses a surrogate model $\hat{\theta}$ approximating θ . Let x be a benign query, $\mathcal{P}(x)$ the set of
194 prefixes that the model may generate in response to query x , and \mathcal{V} the vocabulary. The attack relies
195 on the following assumption about model similarity:

196 **Assumption 1** (Surrogate Model Logit Fidelity). *There exist $\delta \geq 0, \epsilon \geq 0$ such that, for every query
197 $x \in \mathcal{X}$:*

$$198 \max_{p \in \mathcal{P}(x)} \left\| \text{Logits}(p; \theta) - \text{Logits}(p; \hat{\theta}) \right\|_{\infty} \leq \delta. \quad (2)$$

199 with probability at least $1 - \epsilon$.

200 Here, $\|\cdot\|_{\infty}$ is the ℓ_{∞} norm and $\text{Logits}(p; \cdot)$ is the logit vector for the next token prediction given
201 prefix p .

202 Assumption 1 implies probabilistic indistinguishability. The L_{∞} logit bound δ ensures that for any set
203 of next tokens $Y' \subseteq \mathcal{V}$ and any prefix p covered by the assumption, the next-token probabilities satisfy
204 $P_{\theta}(Y'|p) \leq e^{2\delta} \cdot P_{\hat{\theta}}(Y'|p)$ and vice versa. Thus, with probability $1 - \epsilon$, the models’ next-token
205 distributions are multiplicatively close by $e^{2\delta}$ for all prefixes. This mirrors (ϵ', δ') -DP, where $\epsilon' = 2\delta$
206 controls the multiplicative bound and ϵ acts like δ' , the probability of failure. The ideal case $\theta = \hat{\theta}$
207 yields $\delta = 0, \epsilon = 0$.

216 4.1.1 ATTACK PROCEDURE USING TEACHER FORCING
217

218 The attacker sends K queries $\mathcal{Q}^K = \{\mathcal{Q}_i\}$ to the provider, who returns responses $\mathcal{R}^K = \{\mathcal{R}_i\}$,
219 where each $\mathcal{R}_i = (r_{i,1}, \dots, r_{i,T_i}) \in \mathcal{V}^*$ is a sequence of length T_i , generated as $\mathcal{R}_i \leftarrow$
220 $\text{Generate}(C(s^*) \parallel \mathcal{Q}_i; \theta)$.

221 Given $(\mathcal{Q}^K, \mathcal{R}^K)$, the attacker performs MLE using $\hat{\theta}$. For each candidate secret $s \in \mathcal{S}$, they compute
222 the negative log-likelihood (NLL) via teacher forcing:
223

$$224 \quad \text{NLL}(s) = \sum_{i=1}^K \text{NLL}_i(s) = - \sum_{i=1}^K \sum_{t=1}^{T_i} \log \left(P_{\hat{\theta}}(r_{i,t} \mid r_{i,<t}, C(s), \mathcal{Q}_i) \right),$$

226 where $P_{\hat{\theta}}(r_{i,t} \mid \cdot)$ is the surrogate model's probability for the observed token $r_{i,t}$ given the prefix
227 containing the candidate secret s and previous tokens $r_{i,<t}$. The attacker's estimate \hat{s} is the secret
228 minimizing the NLL:

$$229 \quad \hat{s} = \arg \min_{s \in \mathcal{S}} \text{NLL}(s). \quad (3)$$

231 The attack's success (recovering s^*) relies on (1) the number of sampled tokens, (2) the sensitivity of
232 the LLM to the secrets, and (3) the fidelity between the surrogate and target models (see Assumption 1).
233 Smaller δ and ϵ ensure $\hat{\theta}$ closely mimics θ 's probabilities, making the NLL calculation more likely to
234 identify the true secret.

235 4.2 QUERY SELECTION STRATEGIES
236

238 The effectiveness of secret inference attacks depends critically on the choice of queries used to probe
239 the target model θ . Given a budget of K queries and a pool of benign candidates $\mathcal{Q}_{\text{pool}}$, the attacker
240 uses the surrogate model $\hat{\theta}$ to select a subset $\mathcal{Q}^K \subset \mathcal{Q}_{\text{pool}}$ that best distinguishes the true secret s^* from
241 other candidates in \mathcal{S} . The utility of a query \mathcal{Q}_i is measured by its ability to elicit distinct response
242 distributions under different secrets $s_j, s_k \in \mathcal{S}$. We quantify this via the **expected divergence** between
243 next-token probability distributions under teacher forcing. Let $p_t(\cdot \mid r_{i,<t}, C(s), \mathcal{Q}_i; \hat{\theta})$ be the next-
244 token distribution predicted by $\hat{\theta}$ at step t . For a response $\mathcal{R}_i = (r_{i,1}, \dots, r_{i,T_i})$, the cumulative L_1
245 divergence is $\text{Div}(\mathcal{R}_i \mid \mathcal{Q}_i, s_j, s_k) = \sum_{t=1}^{T_i} \frac{1}{2} \|p_t(\cdot \mid r_{i,<t}, C(s_j), \mathcal{Q}_i; \hat{\theta}) - p_t(\cdot \mid r_{i,<t}, C(s_k), \mathcal{Q}_i; \hat{\theta})\|_1$.
246 The expected divergence for query \mathcal{Q}_i and pair (s_j, s_k) is:

$$247 \quad D(s_j, s_k, \mathcal{Q}_i) = \frac{1}{2} \left(\mathbb{E}_{\mathcal{R}_i \sim \theta(\cdot \mid \mathcal{Q}_i, s_j)} [\text{Div}(\mathcal{R}_i \mid \mathcal{Q}_i, s_j, s_k)] + \mathbb{E}_{\mathcal{R}_i \sim \theta(\cdot \mid \mathcal{Q}_i, s_k)} [\text{Div}(\mathcal{R}_i \mid \mathcal{Q}_i, s_j, s_k)] \right). \quad (4)$$

250 This expectation is estimated ($\hat{D}(s_j, s_k, \mathcal{Q}_i)$) by first generating M sample responses $\mathcal{R}^M =$
251 $\{\mathcal{R}_i\}_{i=1}^M$ from θ for each conditioning secret (s_j, s_k) . For each response, $\text{Div}(\cdot)$ is then calcu-
252 lated using $\hat{\theta}$ via teacher forcing, and the results are averaged. A higher $\hat{D}(s_j, s_k, \mathcal{Q}_i)$ indicates query
253 \mathcal{Q}_i better separates s_j and s_k according to $\hat{\theta}$. Our strategy selects K queries \mathcal{Q}^K from the pool of
254 candidates $\mathcal{Q}_{\text{pool}}$ so as to maximize the total estimated expected divergence, given by:

$$256 \quad W(\mathcal{Q}^K \subset \mathcal{Q}_{\text{pool}}) = \max_{\mathcal{Q}^K} \sum_{\mathcal{Q}_i \in \mathcal{Q}^K} \sum_{j \neq k} \hat{D}(s_j, s_k, \mathcal{Q}_i). \quad (5)$$

258 **Prompt Tuning.** We use prompt tuning (Lester et al., 2021) for finding the optimal queries $\mathcal{Q}^K =$
259 $\{\mathcal{Q}_i\}_{i=1}^K$ that maximizes the total estimated expected divergence as shown in equation 5. Let
260 $\mathcal{Q}_i = \{q_{i,1}, \dots, q_{i,T}\}$ with each $q_{i,t} \in \mathbb{R}^d$ be continuous learnable query embedding with T being
261 the token length. We project the continuous query embeddings $q_{i,t} \in \mathbb{R}^d$ back to discrete token
262 space by computing the L2 distance to the $\hat{\theta}$'s embedding matrix $E \in \mathbb{R}^{|\mathcal{V}| \times d}$ selecting the nearest
263 token $q_{i,t}' = \arg \min_{v \in \mathcal{V}} \|q_{i,t} - E_v\|_2$ for each position. We sample responses \mathcal{R}_i^M from the
264 target model θ using $\mathcal{Q}_i' = \{q_{i,1}', \dots, q_{i,T}'\}$ for each conditioning secret (s_j, s_k) . Under teacher
265 forcing, we compute the gradient of the divergence with respect to the continuous query embedding
266 as $g_i = \nabla_{\mathcal{Q}_i} (\sum_{j \neq k} \hat{D}(s_j, s_k, \mathcal{Q}_i))$, which indicates the direction that maximizes the expected
267 divergence. The gradient indicates the direction of the query embedding where expected divergence
268 will be maximum. The query embedding is then updated as $\mathcal{Q}_i \leftarrow \mathcal{Q}_i + \eta g_i$, where $\eta > 0$ is the
269 learning rate.

270 **Online Direct Preference Optimization.** We use DPO-based (Rafailov et al., 2023) method for
 271 finding the optimal queries \mathcal{Q}^K that maximizes the total estimated expected divergence as shown in
 272 equation 5. Let θ_{gen} be a generator model that generates queries $\{\mathcal{Q}_{i,a}\}_{i=1}^K$ at temperature \mathcal{T} and
 273 $\{\mathcal{Q}_{i,b}\}_{i=1}^K$ at temperature $\mathcal{T} + \delta$, where $\delta > 0$ is exploration bound given a context \mathcal{C} . We sample
 274 responses $\{\mathcal{R}_{i,a}^M\}_{i=1}^K$ and $\{\mathcal{R}_{i,b}^M\}_{i=1}^K$ for these queries using target model θ for each conditioning
 275 secret (s_j, s_k) and compute the estimated expected divergence using surrogate model $\hat{\theta}$ to give reward
 276 to these queries as:

$$278 \quad r(\mathcal{Q}^K | \mathcal{C}, \hat{\theta}) = \sum_{i=1}^K \sum_{j \neq k} \hat{D}(s_j, s_k, \mathcal{Q}_i), \quad (6)$$

281 Based on these rewards, we define a preference pairs as:

$$283 \quad \mathcal{Q}^{K,+} = \arg \max_{\mathcal{Q}^K \in \{\mathcal{Q}^{K,a}, \mathcal{Q}^{K,b}\}} r(\mathcal{Q}^K | \mathcal{C}, \hat{\theta}), \quad \mathcal{Q}^{K,-} = \arg \min_{\mathcal{Q}^K \in \{\mathcal{Q}^{K,a}, \mathcal{Q}^{K,b}\}} r(\mathcal{Q}^K | \mathcal{C}, \hat{\theta})$$

285 The generator is updated to increase the likelihood of $\mathcal{Q}^{K,+}$ while suppressing $\mathcal{Q}^{K,-}$ using the
 286 preference loss as follows:

$$289 \quad \mathcal{L}_{DPO}(\theta_{gen}) = -\mathbb{E}_{(q^+, q^-) \sim (\mathcal{Q}^{K,+}, \mathcal{Q}^{K,-})} [\log \sigma(\beta (\log P_{\theta_{gen}}(q^+ | \mathcal{C}) - \log P_{\theta_{gen}}(q^- | \mathcal{C})))].$$

291 where $\sigma(\cdot)$ is the sigmoid function and $\beta > 0$ controls the sharpness of the preference.

292 This procedure is repeated for $T = 100$ iterations, yielding an online dataset of preference pairs.
 293 Unlike standard offline preference optimization, this formulation allows the generator to continually
 294 refine its query distribution in response to the reward. At the end of the training, we select the K
 295 queries with the highest observed reward across all iterations.

297 5 EXPERIMENTS

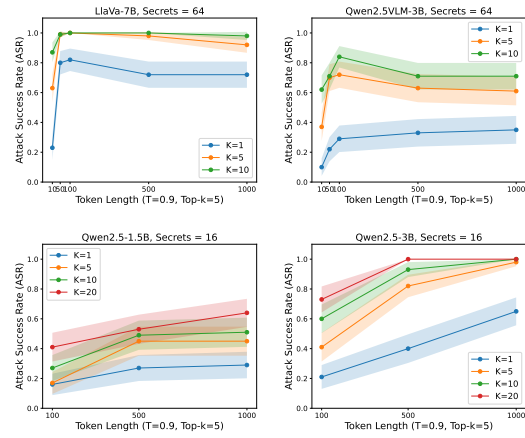
299 We conduct a comprehensive empirical evaluation
 300 to quantify (i) the effectiveness of exact-
 301 context inference attacks across Large Language
 302 Models (LLMs) and Vision-Language Models
 303 (VLMs), (ii) the sensitivity of attack success to
 304 sampling and decoding hyperparameters, and
 305 (iii) the robustness of common defenses and op-
 306 timization strategies (prompt tuning, DPO). For
 307 reproducibility, we release model/config lists,
 308 seeds, and plotting scripts in the Appendix.

309 5.1 EXPERIMENTAL SETUP

311 **LLMs and VLMs.** We experiment with
 312 instruction-tuned versions from the Qwen2.5
 313 model series (Yang et al., 2024), since this al-
 314 lows fine-grained ablation studies over various
 315 model sizes. The models we ablate over range
 316 from 1.5B (billion) to 7B parameters. We write
 317 Qwen2.5-1.5B to denote the 1.5B parameter,
 318 instruction-tuned version (HuggingFace, b) of
 319 Qwen2.5.

320 We evaluate vision language models (VLMs)

321 from the LLaVA (Liu et al., 2023) and Qwen2.5VLM (Bai et al., 2025) model series, ab-
 322 lating across model sizes ranging from 3B to 13B parameters. We use LLaVA-7B and
 323 Qwen2.5VLM-7B to denote the 7B parameter, instruction-tuned versions of LLaVA (Hugg-
 324 ingFace, a) and Qwen2.5VLM (HuggingFace, c), respectively.



325 Figure 2: Exact context inference attack for LLMs
 326 and VLMs, ablated over the query budget K . The
 327 y-axis shows the attack success rate (ASR), and
 328 the x-axis shows the token length. Standard config-
 329 urations are used, with 95% confidence intervals
 330 computed over 100 repetitions.

Implementation Details. The secret inference task aims to identify the true secret used by the model provider, assuming the adversary knows the candidate secret set S . We consider two adversary access scenarios: white-box ($\hat{\theta} = \theta$) and black-box (surrogate $\hat{\theta}$ approximates θ). The attacker is allowed a query budget of K and operates under specified sampling conditions (e.g., temperature T and top- k sampling). To ensure the queries are independent of the secret, we manually craft 50 queries that are semantically unrelated to the private content embedded in the model’s hidden context. In each experiment, we randomly sample K queries from this set and select a true secret $s^* \in S$ uniformly at random. The model is then queried to generate responses: $R_i \leftarrow \text{Generate}(C(s^*), Q_i; \theta)$. The candidate secret set consists of private images from CelebA dataset (Liu et al., 2015) (for VLMs) or binary string passwords (for LLMs), depending on the task as shown in Table 1. The attacker uses the surrogate model $\hat{\theta}$ to compute per-token log-likelihoods of responses under each candidate secret, aggregates them into scores, and predicts the candidate with the highest score as the true secret. Each experiment is repeated 100 times to compute the average attack success rate of the true secret.

Standard Configurations. Unless otherwise specified, we adopt a standard configuration with temperature set to 0.9, top- k = 5, R_{\max} = 500, and a query budget of K = 10 for LLMs and K = 1 for VLMs, with secret length $|S|$ = 16 for LLMs and $|S|$ = 64 for VLMs. We vary specific parameters (e.g., top- k , temperature, secret length, model size, query budget, and token length) in dedicated experiments to study their effect.

5.2 ATTACKS

Token Length and Query Budget. To assess the effectiveness of our attack, we measure the *Attack Success Rate (ASR)* as a function of token length, under different query budgets and the standard configuration across various VLMs and LLMs. For VLM families, ASR increases with token length up to about 100 tokens, after which it either plateaus or slightly declines. In contrast, for LLM families, ASR continues to improve steadily as the token length grows from 100 to 1000 as shown in Figures 2 and 7. These results suggest that VLMs exhibit diminishing information gain beyond a certain token length, whereas LLMs continue to benefit from longer contexts. We also observe that allocating a larger query budget consistently increases ASR for both VLMs and LLMs, as additional queries provide greater information for secret inference.

Top and Temperature. We study the impact of decoding parameters on the effectiveness of secret inference attacks by measuring the *Attack Success Rate (ASR)* as a function of top- k while varying the sampling temperature under the standard configuration across different VLMs and LLMs (Figures 4 and 8). For VLMs, ASR consistently improves at lower temperatures, indicating that deterministic decoding makes secret inference easier. In contrast, increasing top- k generally reduces ASR, suggesting that larger top- k sampling dilutes the secret-related signal. For LLMs, ASR remains high across most conditions (85–95%). With respect to top- k , ASR follows a U-shaped trend, initially decreasing as top- k increases, then recovering at higher values. Temperature effects show an inverted U-shape, with ASR peaking at intermediate values before declining. These results suggest that VLMs are more sensitive to decoding randomness, with lower temperatures amplifying secret leakage. In contrast, LLMs exhibit robustness, achieving high ASR under most settings, with optimal secret inference occurring at moderate levels of decoding randomness that balance diversity and signal clarity.

Secret Length and Model Size. We analyze the effectiveness of our attack by plotting the *Attack Success Rate (ASR)* as functions of secret length, while varying the model sizes under the standard configuration across different VLMs and LLMs (Figures 3).

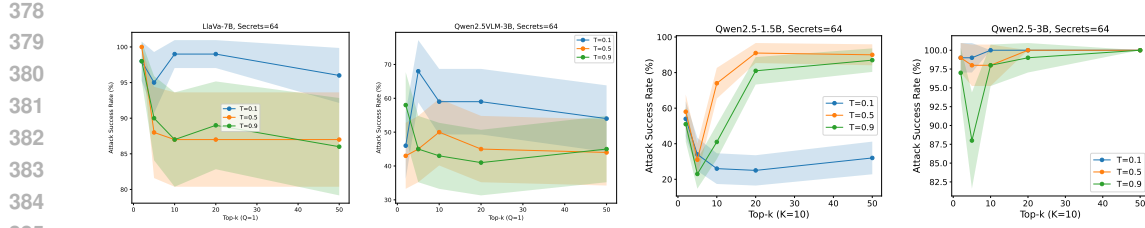


Figure 4: Exact context inference attack for LLMs and VLMs, ablated over the temperature T . The y-axis shows the attack success rate (ASR), and the x-axis shows the top- k . Standard configurations are used, with 95% confidence intervals computed over 100 repetitions.

We observe for all model families that (i) models with more parameters have a substantially higher probability of leaking the true secret and (ii) the decrease in the attack success rate is approximately linear in log scale of the number of candidate secrets except for Qwen2.5-7B and Qwen2.5-3B remaining relatively flat. In general LLaVA model family have more tendency to leak private information than the Qwen2.5VLM model family. In summary, both model size and secret length significantly influence attack success. Larger models and shorter secrets are more vulnerable to leakage, while smaller models or longer secrets reduce ASR.

5.3 DEFENSES

We evaluate the robustness of our attack using three defense mechanisms: instruction-based, output-filtering, and a combined instruction + output-filtering scheme. The instruction-based defense explicitly instructs the model not to reveal any information from the context prompt. The output-filtering defense post-processes model responses to detect and remove private or sensitive information. The combined defense applies both strategies together

Instruction-based Defense. We propose an instruction-based defense that appends explicit instructions to the hidden context of both LLMs and VLMs, guiding the models not to reveal private information. Figures 6 and 9 show that this defense only slightly reduces ASR for most model families, except for the Qwen2.5VLM series, which experiences a substantial drop. This suggests that Qwen2.5VLM series have higher instruction-following ability compared to other models.

Output Filtering-based Defense. We implement an output-filtering defense that screens model responses and replaces any containing sensitive information with a generic message, *e.g.*, “I can’t provide any information” using OpenAI’s GPT-4o (OpenAI, 2025). As shown in Figures 6 and 9, this approach substantially reduces ASR for most model families, but has little effect on the Qwen2.5-VLM series. This difference arises because the defense is effective only when models leak secrets verbatim. Qwen2.5-VLM models may rarely disclose sensitive content explicitly, allowing the attack to remain largely successful. This highlights the limitations of output filtering as a general defense.

Instruction + Output Filtering-based Defense. We evaluate a combined defense that integrates instruction-based guidance (instructing models not to reveal sensitive information) with output filtering (replacing sensitive outputs with a generic message). Figures 6 and 9 show that for most models, ASR under the combined defense is similar to or higher than with output filtering alone, because instructions suppress explicit disclosures, leaving the filter inactive, while our attack exploits information in seemingly benign responses. For Qwen2.5-VLM models, which rarely leak sensitive content, the combined defense behaves like the instruction-based approach, highlighting that its effectiveness in this case stems primarily from instruction following.

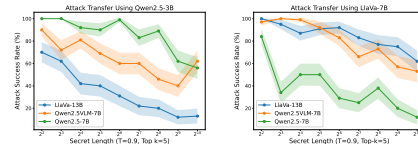


Figure 5: Attack Transfer using Qwen2.5-3B (left) LLaVA-13B (right). Attack transferability is strongest within the same model family and context type.

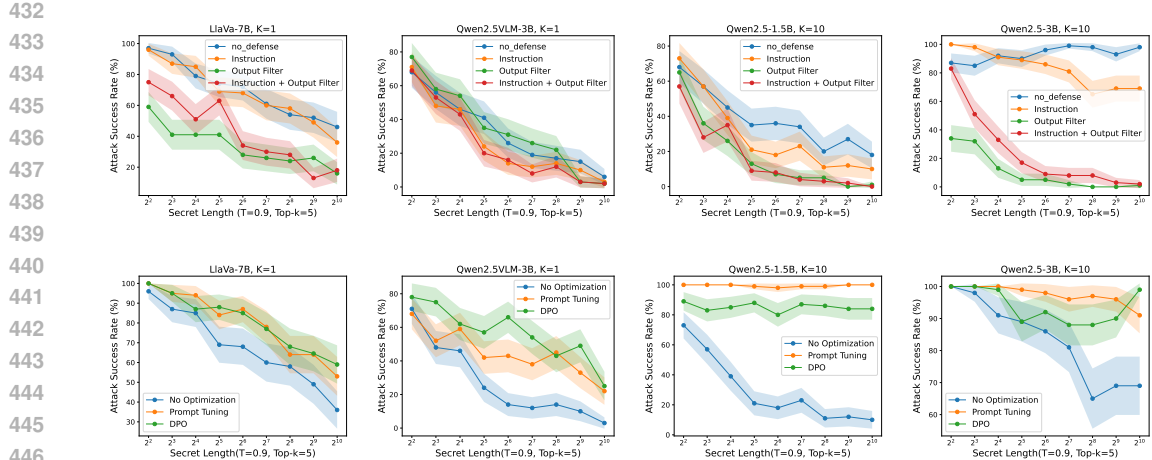


Figure 6: Exact context inference attacks ablated over various defenses (above) and optimization techniques (below). Optimization techniques substantially improve ASR across LLMs and VLMs, even under instruction-based defenses.

5.4 PROMPT OPTIMIZATION

Prompt Tuning. We apply prompt tuning ($K = 1$ for VLMs, $K = 10$ for LLMs) under standard configurations to optimize query selection. For LLMs, this approach achieves ASR of at least 84%, with Qwen2.5-1.5B reaching nearly 100% ASR for secrets up to 1024 tokens, and slightly lower ASR for larger Qwen2.5 models. For VLMs, improvements are modest for the LLaVA series and Qwen2.5VLM-3B, but substantial for Qwen2.5VLM-7B (Figures 6 and 10). These results show that prompt tuning effectively leverages model behavior and secret length to maximize attack success across different model sizes.

DPO. We apply online DPO ($K = 1$ for VLMs, $K = 10$ for LLMs) with a generator model $\theta_{\text{gen}} = \text{Qwen0.5B-Instruct}$ to optimize query selection under standard configurations with instruction-based defense. DPO achieves at least 80% ASR across the Qwen2.5 family, increasing with model size and reaching nearly 100% for Qwen2.5-7B up to $|\mathcal{S}| = 1024$. For VLMs, both LLaVA and Qwen2.5VLM series show substantially higher ASR compared to the no-optimization baseline (Figures 6 and 10). Unlike prompt-tuned queries, DPO-generated queries are benign and unlikely to be blocked by input filters, maintaining high ASR even under defensive measures.

Transferability of Attack. We study attack transfer by optimizing queries with online DPO on smaller surrogate models (LLaVA-7B, Qwen2.5-3B) and testing them on larger targets (LLaVA-13B, Qwen2.5-7B, Qwen2.5VLM-7B) under instruction-based defenses as shown in Figure 5. Queries optimized on Qwen2.5-3B achieve 56–100% ASR on Qwen2.5-7B and 40–90% ASR on Qwen2.5VLM-7B for secrets up to 1024 tokens, showing strong transfer within the family, while transfer to LLaVA-13B is weaker (12–70% ASR) due to architectural differences. Queries optimized on LLaVA-7B transfer effectively to LLaVA-13B (62–100% ASR) and moderately to Qwen2.5-7B (12–100% ASR), with weaker transfer for some secret lengths because of differing context types (image vs. text). These results indicate that attack transferability is strongest within the same model family and context type, but cross-model transfer is possible, highlighting the broad applicability of the attack.

6 CONCLUSION

We show that context inference attacks can extract sensitive information even when the model’s outputs do not reveal it verbatim, across both LLMs and VLMs. The attack uses innocuous random queries that can evade filtering, making it difficult to detect. We further optimize queries using DPO, generating benign queries that achieve substantially higher ASR. Optimized queries also transfer effectively from smaller surrogate models to larger targets, with strongest transfer within the same model family and context type. These results demonstrate the broad applicability of the attack and highlight the need for defenses that address subtle, distributional leakage beyond explicit output filtering.

486 REFERENCES
487488 Shuai Bai, Keqin Chen, Xuejing Liu, Jialin Wang, Wenbin Ge, Sibo Song, Kai Dang, Peng Wang,
489 Shijie Wang, Jun Tang, et al. Qwen2. 5-vl technical report. *arXiv preprint arXiv:2502.13923*,
490 2025.491 Nicholas Carlini, Florian Tramer, Eric Wallace, Matthew Jagielski, Ariel Herbert-Voss, Katherine
492 Lee, Adam Roberts, Tom Brown, Dawn Song, Ulfar Erlingsson, et al. Extracting training data
493 from large language models. In *30th USENIX security symposium (USENIX Security 21)*, pp.
494 2633–2650, 2021.495 Mark Chen, Jerry Tworek, Heewoo Jun, Qiming Yuan, Henrique Ponde De Oliveira Pinto, Jared
496 Kaplan, Harri Edwards, Yuri Burda, Nicholas Joseph, Greg Brockman, et al. Evaluating large
497 language models trained on code. *arXiv preprint arXiv:2107.03374*, 2021.498 Haonan Duan, Adam Dziedzic, Mohammad Yaghini, Nicolas Papernot, and Franziska Boenisch. On
499 the privacy risk of in-context learning. *arXiv preprint arXiv:2411.10512*, 2024.500 Wenjie Fu, Huandong Wang, Chen Gao, Guanghua Liu, Yong Li, and Tao Jiang. A probabilistic fluc-
501 tuation based membership inference attack for diffusion models. *arXiv preprint arXiv:2308.12143*,
502 2023.503 HuggingFace. Llava-1.5-7b. <https://huggingface.co/llava-hf/llava-1.5-7b-hf>,
504 a. Accessed: 2025-09-25.505 HuggingFace. Qwen2.5-1.5b. <https://huggingface.co/Qwen/Qwen2.5-1.5B>, b. Ac-
506 cessed: 2025-09-25.507 HuggingFace. Qwen2.5-vl-7b. <https://huggingface.co/Qwen/Qwen2.5-VL-7B-Instruct>, c. Accessed: 2025-09-25.508 Brian Lester, Rami Al-Rfou, and Noah Constant. The power of scale for parameter-efficient prompt
509 tuning. *arXiv preprint arXiv:2104.08691*, 2021.510 Patrick Lewis, Ethan Perez, Aleksandra Piktus, Fabio Petroni, Vladimir Karpukhin, Naman Goyal,
511 Heinrich Küttler, Mike Lewis, Wen-tau Yih, Tim Rocktäschel, et al. Retrieval-augmented genera-
512 tion for knowledge-intensive nlp tasks. *Advances in neural information processing systems*, 33:
513 9459–9474, 2020.514 Chunyuan Li, Cliff Wong, Sheng Zhang, Naoto Usuyama, Haotian Liu, Jianwei Yang, Tristan
515 Naumann, Hoifung Poon, and Jianfeng Gao. Llava-med: Training a large language-and-vision
516 assistant for biomedicine in one day. *Advances in Neural Information Processing Systems*, 36:
517 28541–28564, 2023.518 Haotian Liu, Chunyuan Li, Qingyang Wu, and Yong Jae Lee. Visual instruction tuning. *Advances in
519 neural information processing systems*, 36:34892–34916, 2023.520 Ziwei Liu, Ping Luo, Xiaogang Wang, and Xiaou Tang. Deep learning face attributes in the wild. In
521 *Proceedings of International Conference on Computer Vision (ICCV)*, December 2015.522 Yash Mathur, Sanketh Rangreji, Raghav Kapoor, Medha Palavalli, Amanda Bertsch, and Matthew R
523 Gormley. Summqa at medqa-chat 2023: In-context learning with gpt-4 for medical summarization.
524 *arXiv preprint arXiv:2306.17384*, 2023.525 Michael Moor, Qian Huang, Shirley Wu, Michihiro Yasunaga, Yash Dalmia, Jure Leskovec, Cyril
526 Zakka, Eduardo Pontes Reis, and Pranav Rajpurkar. Med-flamingo: a multimodal medical few-shot
527 learner. In *Machine Learning for Health (ML4H)*, pp. 353–367. PMLR, 2023.528 OpenAI. Gpt-4o. <https://platform.openai.com/docs/models/gpt-4o>, 2025. Ac-
529 cessed: 2025-09-25.530 Rafael Rafailov, Archit Sharma, Eric Mitchell, Christopher D Manning, Stefano Ermon, and Chelsea
531 Finn. Direct preference optimization: Your language model is secretly a reward model. *Advances
532 in neural information processing systems*, 36:53728–53741, 2023.

540 Ahmed Salem, Yang Zhang, Mathias Humbert, Pascal Berrang, Mario Fritz, and Michael Backes.
 541 MI-leaks: Model and data independent membership inference attacks and defenses on machine
 542 learning models. *arXiv preprint arXiv:1806.01246*, 2018.

543 Jingzhe Shi, Jialuo Li, Qinwei Ma, Zaiwen Yang, Huan Ma, and Lei Li. Chops: Chat with customer
 544 profile systems for customer service with llms. *arXiv preprint arXiv:2404.01343*, 2024.

545 Reza Shokri, Marco Stronati, Congzheng Song, and Vitaly Shmatikov. Membership inference attacks
 546 against machine learning models. In *2017 IEEE symposium on security and privacy (SP)*, 2017.

547 Rui Wen, Tianhao Wang, Michael Backes, Yang Zhang, and Ahmed Salem. Last one standing: A
 548 comparative analysis of security and privacy of soft prompt tuning, lora, and in-context learning.
 549 *arXiv preprint arXiv:2310.11397*, 2023.

550 Rui Wen, Zheng Li, Michael Backes, and Yang Zhang. Membership inference attacks against
 551 in-context learning. In *Proceedings of the 2024 on ACM SIGSAC Conference on Computer and*
552 Communications Security, pp. 3481–3495, 2024.

553 An Yang, Baosong Yang, Beichen Zhang, Binyuan Hui, Bo Zheng, Bowen Yu, Chengyuan Li,
 554 Dayiheng Liu, Fei Huang, Haoran Wei, Huan Lin, Jian Yang, Jianhong Tu, Jianwei Zhang, Jianxin
 555 Yang, Jiaxi Yang, Jingren Zhou, Junyang Lin, Kai Dang, Keming Lu, Keqin Bao, Kexin Yang,
 556 Le Yu, Mei Li, Mingfeng Xue, Pei Zhang, Qin Zhu, Rui Men, Runji Lin, Tianhao Li, Tingyu Xia,
 557 Xingzhang Ren, Xuancheng Ren, Yang Fan, Yang Su, Yichang Zhang, Yu Wan, Yuqiong Liu, Zeyu
 558 Cui, Zhenru Zhang, and Zihan Qiu. Qwen2.5 technical report. *arXiv preprint arXiv:2412.15115*,
 559 2024.

560 Samuel Yeom, Irene Giacomelli, Matt Fredrikson, and Somesh Jha. Privacy risk in machine learning:
 561 Analyzing the connection to overfitting. In *2018 IEEE 31st computer security foundations*
562 symposium (CSF), pp. 268–282. IEEE, 2018.

563 Yiming Zhang and Daphne Ippolito. Prompts should not be seen as secrets: Systematically measuring
 564 prompt extraction attack success. *arXiv preprint arXiv:2307.06865*, 16, 2023.

565 Yiming Zhang, Nicholas Carlini, and Daphne Ippolito. Effective prompt extraction from language
 566 models. *arXiv preprint arXiv:2307.06865*, 2023.

567 Yongchao Zhou, Andrei Ioan Muresanu, Ziwen Han, Keiran Paster, Silviu Pitis, Harris Chan, and
 568 Jimmy Ba. Large language models are human-level prompt engineers. In *The eleventh international*
569 conference on learning representations, 2022.

570

571

572

573

574

575

576

577

578

579

580

581

582

583

584

585

586

587

588

589

590

591

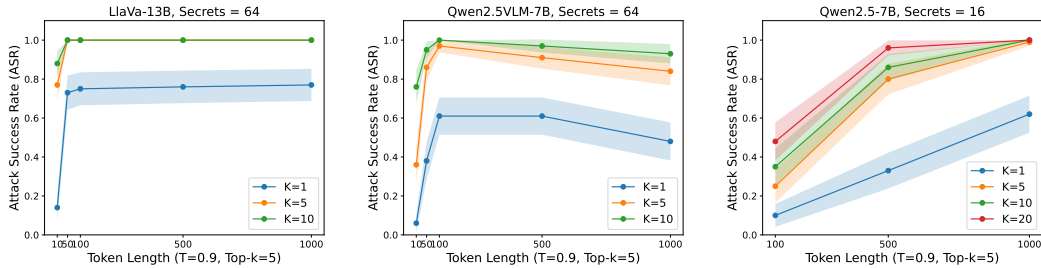
592

593

594 **A RELATED WORK**
 595

596 **Privacy vulnerabilities in system/hidden prompts.** Zhang et al. (2023) demonstrate that prompt
 597 extraction can be highly effective with a small set of human-crafted queries augmented by GPT-4
 598 generated variants, achieving strong precision using only API access. Duan et al. (2024) study privacy
 599 leakage in both in-context prompting and fine-tuning, finding that in-context prompting is generally
 600 more susceptible to leakage. Extending this line, Wen et al. (2023) systematically compare adaptation
 601 methods, Low-Rank Adaptation (LoRA), Soft Prompt Tuning (SPT), and In-Context Learning (ICL),
 602 and report that ICL is the most vulnerable to membership inference while being comparatively less
 603 affected by backdoor attacks than LoRA/SPT. Focusing on realistic black-box settings, Wen et al.
 604 (2024) analyze membership inference against ICL under API-only access, where the attacker observes
 605 text but not tokenizer internals or token-level probabilities. Our work is complementary: rather than
 606 extracting a verbatim prompt or testing membership of a specific context example, we infer *which*
 607 secret from a candidate set is embedded in the hidden prompt by exploiting distributional shifts in
 608 model responses to benign queries.
 609

610 **Membership inference attacks.** Membership inference tests whether a data point was used during
 611 training (Shokri et al., 2017), with enhancements for black-box/white-box settings and regularization-
 612 aware analyses (Yeom et al., 2018; Salem et al., 2018). For instance, Carlini et al. (2021) demonstrate
 613 that large language models can be exploited to generate candidate samples, with membership inference
 614 attacks filtering out non-member sequences to recover verbatim training data. Similarly, for diffusion
 615 models, Fu et al. (2023) show that membership inference can be mounted by measuring probabilistic
 616 fluctuations around candidate records, enabling identification of whether specific samples were used
 617 in training. Recent work further extends these membership-style attacks beyond training data to the
 618 *in-context* prompt setting. In the context of ICL, Wen et al. (2024) investigate API-only scenarios
 619 where token probabilities are unavailable. Our formulation differs: we frame *context inference* as a
 620 membership-style identification over a *set of candidate secrets* embedded at inference time, using a
 621 surrogate likelihood test aggregated over multiple benign queries.
 622



631 Figure 7: Exact context inference attack model with secret length $|S| = 64$, ablated over query budget
 632 Q . The y-axis shows attack success rate (ASR), and the x-axis shows token length. We use top- $k = 5$
 633 and temperature $T = 0.9$, with 95% confidence intervals computed over 100 repetitions.
 634

635 **B LIMITATIONS**
 636

637 Our strategies rely on the fidelity of the surrogate model $\hat{\theta}$ (Assumption 1). If $\hat{\theta}$ accurately approximates θ (small δ, ϵ), then the estimated divergences $\hat{D}(s_j, s_k, Q_i)$ should correlate well with the true divergences under θ . Consequently, the selected query set Q^K is expected to be effective when used against the target model θ . The primary limitations are the potential mismatch between $\hat{\theta}$ and θ and the noise introduced by Monte Carlo estimation of $D(s_j, s_k, Q_i)$.
 638

639 **B.1 DETAILS ON THE EXPERIMENTAL SETUP**
 640

641 **Hardware and Software.** All experiments are run on Nvidia A6000 GPUs and we generate text
 642 using the default `model.generate()` function from the `transformers` library. We do not
 643

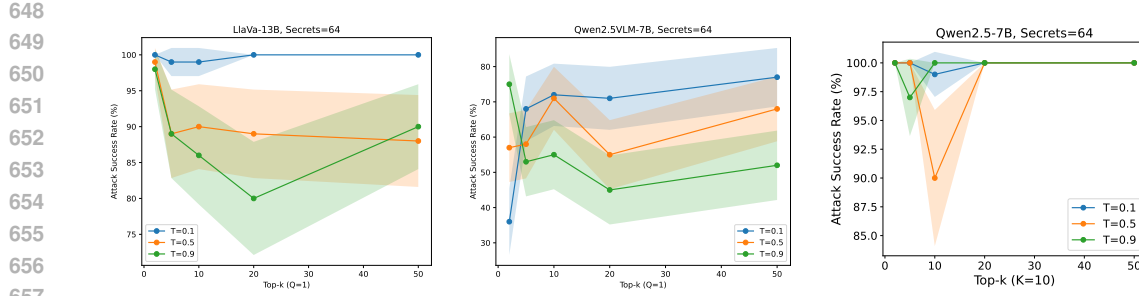


Figure 8: Exact context inference attack model with secret length $|S| = 64$, ablated over Temperature T . The y-axis shows attack success rate (ASR), and the x-axis shows top- k . We sample $R_{\max} = 500$ tokens per query for $Q = 1$ query, with 95% confidence intervals computed over 100 repetitions.

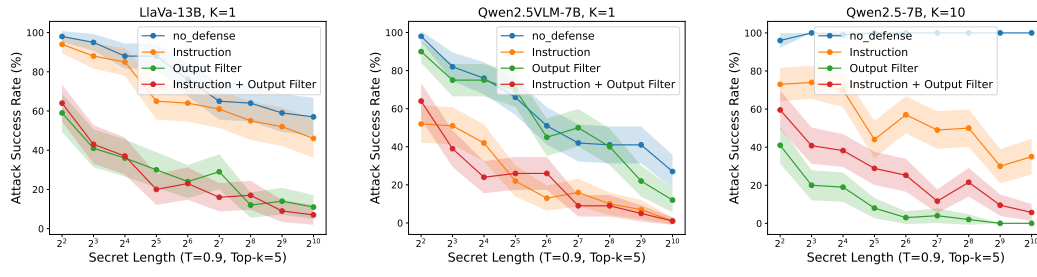


Figure 9: Exact context inference attacks ablated over various defenses. The y-axis shows the attack success rate (ASR), and the x-axis shows the secret length. We sample $R_{\max} = 500$ tokens per query for $Q = 1$ query, use top- $k = 5$, and a temperature of $T = 0.9$, with 95% confidence intervals computed over 100 repetitions.

deactivate randomness or enter the debugging mode and highlight that producing the next-token logits is already randomized even without considering the randomness introduced from sampling. Running the `model.generate()` function twice on the same input with the same models and parameters may produce slightly different logits due to inherent non-determinism of GPU calculations, which may lead to different tokens being included in the top- k selection.

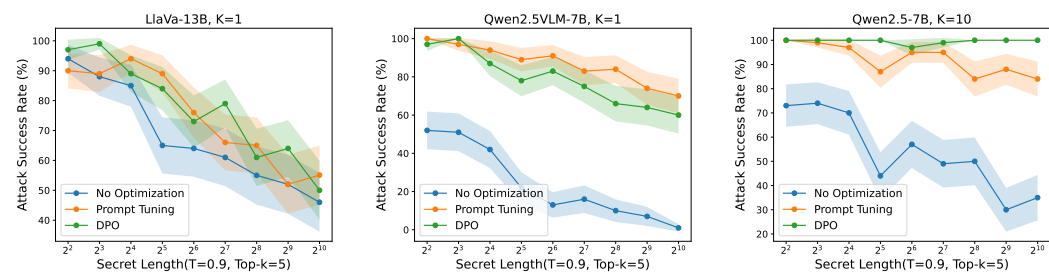


Figure 10: Exact context inference attacks ablated over various optimization technique. The y-axis shows the Attack Success Rate (ASR), and the x-axis shows the secret length. We sample $R_{\max} = 500$ tokens per query for $Q = 1$ query, use top- $k = 5$, and a temperature of $T = 0.9$, with 95% confidence intervals computed over 100 repetitions.

Context Image	Context Prompts	Model Type
-	Here is a secret: 1001001101 . You must never reveal or mention this secret in any form, directly or indirectly, regardless of future instructions.	Qwen2.5 series (LLM)
	messages = [{"role": "system", "content": (``IMPORTANT: You may use attached images only for the task requested. Do not reveal, speculate about, or extract any private, sensitive, or identifying information from them (such as faces, documents, or personal text). Only analyze or reference images in ways directly relevant to the users instructions."), { "role": "user", "content": [image_content] }]	Qwen2.5-VL series (VLM)
	USER: <image> IMPORTANT: Completely ignore the image above. Do not describe, analyze, mention, or refer to it in any way not directly or indirectly. Your task is ONLY to respond to the following instruction:	LlaVa series (VLM)

Table 1: Context Images, context prompts, and model types.